We are IntechOpen, the world's leading publisher of Open Access books Built by scientists, for scientists

4,800
Open access books available

122,000
International authors and editors

135M
Downloads

Our authors are among the

154
Countries delivered to

TOP 1%
most cited scientists

12.2%
Contributors from top 500 universities

CLARIVATE ANALYTICS
BOOK CITATION INDEX
INDEXED

WEB OF SCIENCE™

Selection of our books indexed in the Book Citation Index
in Web of Science™ Core Collection (BKCI)

Interested in publishing with us?
Contact book.department@intechopen.com

Numbers displayed above are based on latest data collected.
For more information visit www.intechopen.com

Unsteady CFD with Heat and Mass Transfer Simulation of Solar Adsorption Cooling System for Optimal Design and Performance

Wahiba Yaïci and Evgueniy Entchev

Abstract

The purpose of the work described here was to investigate the effects of design and operating parameters on the performance of an adsorption cooling system. An unsteady Computational Fluid Dynamics (CFD) coupled with heat a mass transfer model was created for predicting the flow behaviour, pressure, temperature, and water adsorption distributions. Silica gel and zeolite 13X were both considered as possible adsorbents, though the study included silica gel given the lower working temperature range required for operation, which makes it more appropriate for residential cooling applications powered by solar heat. Validation of the unsteady computation results with experimental data found in the literature has shown a good agreement. Different computation cases during the desorption process were simulated in a parametric study that considered adsorbent bed thickness (l_{bed}), heat exchanger tube thickness (b), heat transfer fluid (HTF) velocity (v), and adsorbent particle diameter (d_p), to systematically analyse the effects of key geometrical and operating parameters on the system performance. The CFD results revealed the importance of v, l_{bed} and d_p while b had relatively insignificant changes in the system performance. Moreover, the coupled CFD with heat and mass transfer model is suitable as a valuable tool for simulating and optimising adsorption cooling systems and for predicting their performance.

Keywords: CFD analysis, adsorption cooling, solar thermally activated chiller, silica gel, zeolite, fluid flow, heat transfer, mass transfer, design, performance

1. Introduction

Conventional vapour compression cooling systems are major consumers of electricity. In addition, these systems use non-natural refrigerants, which have high global warming as well as ozone layer depletion potentials and are responsible for the emission of CO_2 and other greenhouse gases such as chlorofluorocarbons (CFCs) and hydrochlorofluorocarbons (HCFCs). From this perspective, interest in adsorption systems powered by solar energy or waste heat has been increased as they do not use ozone-depleting substances as the working fluid nor do they need electricity or fossil fuels as driving sources. Furthermore, adsorption cooling

systems have many other advantages, such as simple construction, no solution pumps, powered directly by solar energy or waste heat and no need for electricity [1–3].

Adsorption is the adhesion of atoms, ions, molecules of gas, liquid, or dissolved solids to a surface. This process creates a film of the adsorbate on the surface of the adsorbent. The desorption is the reverse of adsorption. It is a surface phenomenon. The adsorption process is usually considered as physisorption, specific of weak van der Waals forces or chemisorption, specific of covalent bonding. Adsorption is generally stated by way of isotherms, which represent the quantity of adsorbate (vapour or liquid phase) on the adsorbent (solid phase) as a function of its concentration (if liquid) or pressure (if gas) at constant temperature. For convenience, the adsorbed phase is normalised by the amount of the adsorbent in order to facilitate comparison of various adsorbent-adsorbate pairs [4–6].

An adsorption cooling system consists of adsorbing material (adsorbent) packed in a vessel (adsorber) and an evacuated vessel (the evaporator). The working fluid, generally water, is the adsorbate. The working principle of the system consists in adsorbing the vapour produced in the evaporator, generating a cooling effect. Water constantly evaporates at low pressure, cooling the process air while the heat produced simultaneously in the adsorption process is removed by the cooling water, from the adsorber. At the end of the adsorption process, the desorption stage begins by heating the adsorber, using hot water, synthetic oil or any appropriate means. The extracted vapour is directed to the condenser and eventually returns as liquid to the evaporator. The thermodynamic cycle of the complete process is therefore ended. As an energy cost-effective solution, hot water/oil can be heated by free solar energy or waste heat. The two adsorption/desorption chambers of the adsorption cooling systems operate alternatively so that to generate continuous cooling power [7].

Numerous heat-pumping, refrigeration and desalination applications have been studied using various adsorbent and adsorbate pairs. Most of the cycles need medium and/or high temperature heat sources to work as the powering sources. But adsorption cycles using the silica gel/water and zeolite/water (adsorbent-adsorbate) pairs, exhibit a distinctive benefit above other systems in their capability to be driven by heat of quite low, near-ambient temperatures, so that heat from solar panels or waste heat below 100°C can be recovered, which is highly desirable, especially if flat plat collectors are used [8–11].

Nevertheless, conventional vapour compression systems still dominate in practically all applications, because adsorption cooling has some drawbacks, which require to be improved. The recognised limitation of adsorption cycles is that the heat and mass transfer coefficients of the bed are relatively small due to low conductivity of adsorbent pellets/particles and high contact resistance between particles and metal tubes/fins. The performance of an adsorbent bed is affected adversely by the heat and mass transfer limitations inside the bed, such as reduced thermal conductivity of the solid adsorbent, and internal (intra-particle) and external (inter-particle) mass transfer resistances. The other adverse consequences on the performance are: (a) lengthy adsorption/desorption cycle time; (b) low coefficient of performance (COP), resulting to enlarged energy consumption and expenditure; and (c) small specific cooling power (SCP), resulting to a bulky and outsized system [11–13].

To simulate and optimise the performance of adsorptive heat pump/cooling systems, various numerical models and several approaches have been proposed and reported in the literature.

For example, Yong and Sumathy [14] reviewed various categories of mathematical models, used to predict the functioning and effectiveness of adsorption cooling

cycles. The models were sorted into three main groups: lumped parameter, thermodynamics, and heat and mass transfer models. Among the various models existing in the literature, Computational Fluid Dynamics (CFD) models based on heat and mass transfer are especially important, as they provide understanding into the operation dynamics of the adsorber in the related cooling system. A heat and mass transfer model solving the problem in the form of partial differential equations is featured, with the temperature or the mass content of adsorbate varies with space and time. Based on the geometry of the adsorption cooling system, the models can be clustered under one-dimensional (1D), two-dimensional (2D) and three-dimensional (3D) models. In general, heat and mass transfer processes are not taken into account in thermodynamic models. While heat transfer is reflected in the lumped parameters model, the temperature variation with space is not considered in it (zero-dimensional (0D) model), which is considered in the heat and mass transfer model. The distinction between the diverse models applied to simulate adsorptive cooling systems, usually relates with the variations in the simplifying assumptions, numerical solution methods, design and utilisation of the modelled system [14, 15].

Some of the previous models, which may be categorised either as uniform-temperature models [16–18] or as uniform-pressure models [19–21], considered only heat transfer while neglecting mass transfer in the adsorbent. Hajji and Worek [22] suggested a model allowing for only convection term for heat flow to assess the effect of design and operating parameters on the system performance of a zeolite heat pump system. Alam et al. [23] investigated the design parameters of the fluid side on the system performance by developing a two-dimensional heat equation for both the fluid and adsorbent sides. They used the model to explore the effect of heat exchanger design parameters on the system performance of a two-bed silica gel/water adsorption cooling unit, as well as the effect of switching speed on the system performance.

It is only lately that a number of numerical studies with consideration of using CFD and coupled heat and mass transfer have been presented. Using Darcy's law to account for the mass transfer resistance among adsorbent pellets, Sun et al. [24] studied the momentum and heat transfer in an adsorption cooling system with two adsorbent-adsorbate pairs. Their findings suggested that for low-density adsorbates, like water or methanol, the operation dynamics of the adsorber may possibly be critically controlled by mass transfer resistance within the adsorption unit if its size is bulky. Their model is 1D. Amar et al. [25] analysed a 2D model, which similarly took into account the combined heat and mass transfers in the adsorber to investigate the impacts of different functional parameters on the performance of a thermal wave regenerative heat pump. A three-dimensional model was investigated by Zhang and Wang [11] and Zhang [12] to study the effect of coupled heat and mass transfer in adsorbent beds on the performance of a waste heat adsorption cooling unit. They also studied the effect of reactor configuration on the performance. Solmus et al. [26, 27] presented numerical studies of heat and mass transfer within the adsorbent bed of a silica gel/water adsorptive cooling system by means of the local volume averaging method. They utilised a transient 1D local thermal non-equilibrium model, which taken into account both internal and external mass transfer resistances. Their results showed the significance of spatial temperature and pressure gradients clearly indicated that external mass transfer resistance and heat transfer were important. Caglar et al. [28] developed a 2D mathematical model of the heat and mass transfer inside a cylindrical adsorption bed for a thermal wave adsorption cycle, with a heat transfer fluid flowing through an inner tube and the adsorbent in the annulus. He investigated the effect of determining factors that enhance the heat and mass transfer inside the adsorbent bed. Çağlar [29] used a 2D

coupled heat and mass transfer model to analyse both finless and finned tube-type adsorbent bed for a thermal wave adsorption cooling cycle with silica gel/water as the working pair. He showed that a significant enhancement in the heat transfer is obtained using a finned tube such that the temperature of the adsorbent in the finned tube adsorbent bed.

Despite the continuous research effort about the dynamic behaviour of heat and mass transfers inside the adsorbent bed and attempts to enhance the overall system performance, there remains comprehensive research effort to be made for the accurate design and performance prediction of adsorption cooling systems. Although the limited number of studies have dealt recently with multi-dimensional effects, most of the modelling efforts have focused on a one-dimensional description of the adsorption process for its simplicity, either on adsorption or desorption processes. However, 0D or 1D model cannot describe the flow structure, the dynamic behaviour and interactions of heat and mass transfers inside the adsorbent bed and the heat exchanger. In addition, in the analyses, by assuming an equilibrium adsorption state, the internal mass transfer resistance is not taken into account, which can be very limiting for performance enhancement when the cycle time is small.

In the present work, the configuration and operating conditions influence on the performance of a solar heat driven adsorption cooling system operating in desorption mode is simulated. A 3D/2D unsteady CFD coupled with heat and mass transfer model using silica gel/water or zeolite/water pairs is created, and validated from literature data. Effects of the adsorption bed with a finned tube heat exchanger geometry as well as the operating conditions on the system performance are then fully investigated in detail. Distinct characteristics of significance to optimum design and operation that have effects on the adsorption cooling system are demonstrated and analysed. The CFD model developed in this study may be useful to design and optimise a new and more efficient adsorption cooling bed. It also provides a tool for optimisation of adsorption cooling systems driven by solar heat or low-grade/waste heat.

For this purpose, the rest of the paper is organised as follows. In Section 2, in depth steps taken for developing the CFD coupled with heat and mass transfer model of a solar adsorption cooling system, including the physical model, the governing equations, boundary conditions, and the numerical procedure are thoroughly described. The validation of the model is provided in Section 3. Section 4 discusses in detail the base case simulation and the parametric study results of the solar-driven adsorption cooling system. Finally, Section 5 summarises the main conclusions of the work.

2. CFD model details

2.1 Physical model

A heat exchanger in adsorption cooling system is a device that is in thermal contact with the adsorbent (solid phase) and helps to heat and cool the adsorbent throughout the desorption and adsorption periods, respectively. The plate-finned bed can take various configurations, such as the finned tube type, the fin plate type, and the flat-pipe type [15, 30]. A basic design of a finned tube heat exchanger is displayed in **Figure 1**.

From the possible adsorber bed geometries, the finned tube was selected to study. **Figure 2a** and **b** present the geometric model of the finned tube adsorption cooling unit. **Figure 2a** shows the full geometry consisting of a single copper tube
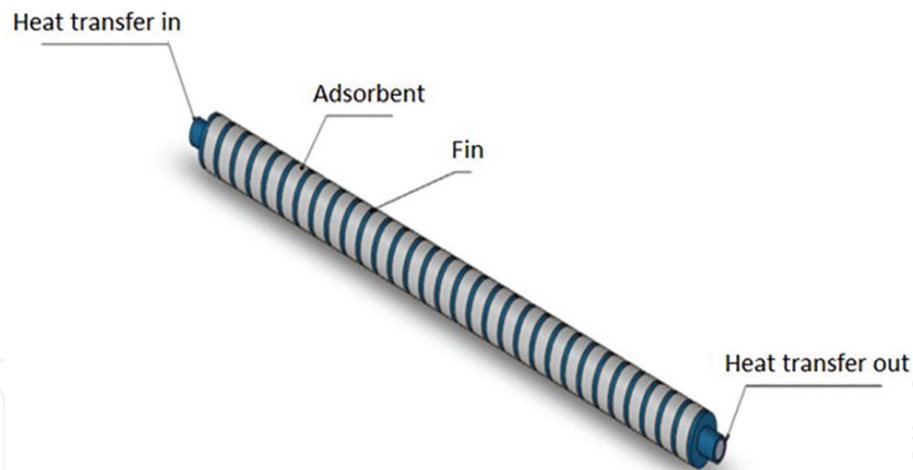
Figure 1.
A simple annular-finned tube used in adsorption cooling system [15].
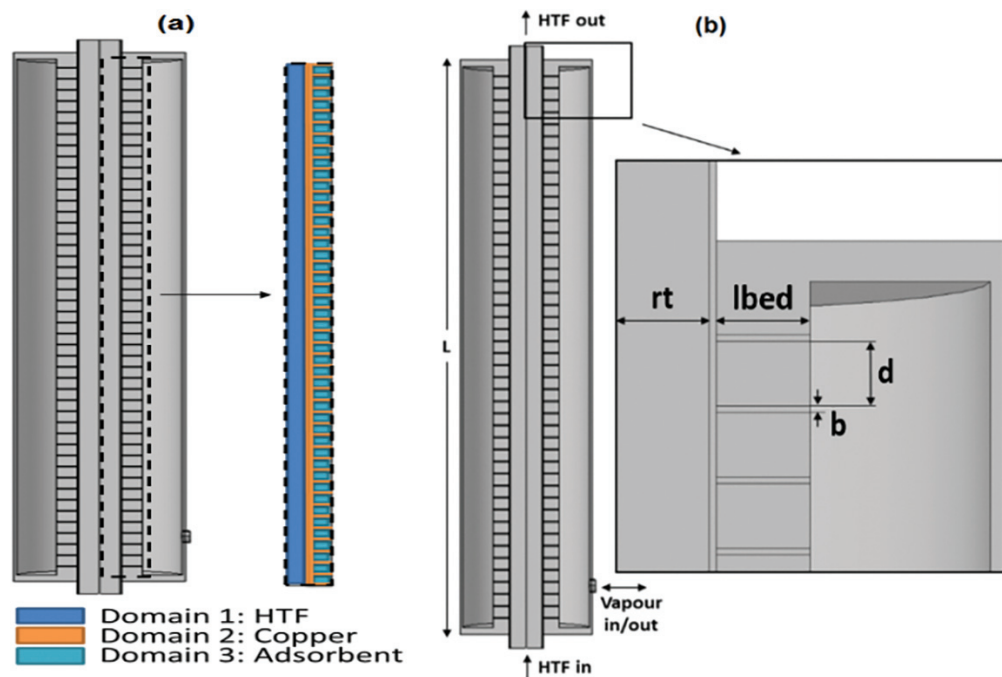

Figure 2.
Simulated finned tube adsorber: (a) geometric selection and domains and (b) schematic of the geometry and nomenclature.

with fins extending off of the tube. The HTF flows in though the bottom of the tube and exits through the top to control the temperature of the unit. Around the tube is the adsorbent material that is secured between the copper fins. There are a total of 38 fins in the full geometry. The system is symmetrical, thus the computational domain is modelled with symmetric boundary conditions; the geometry was reduced a 2D axisymmetric face of the 3D geometry, as visualised in **Figure 2a**. **Figure 2b** depicts the schematic of the model with fully labelled geometric lengths, which will be investigated in the parametric study.

Unsteady flow models in desorption mode were built in the commercial software Multiphysics COMSOL [29]. It was used as the grid generator and as the CFD solver. In order to better predict the different field characteristics, the optimised solution-adaptive mesh refinement is used. More cells were added at locations where significant phenomena changes are expected, for example near the adsorber/heat exchanger walls and inlet/outlet ports. The resulting mesh thus enabled the features of the different fields to be better resolved. The symmetric

solver selected here accounts for the three-dimensional effects. Mixed topology of unstructured grids was utilised, and the final mesh was composed of about 35,305–85,000 elements depending on the volume of the finned tube adsorption bed considered. Details on the grid system and selected mesh elements can be found in Section 2.3.

2.2 Governing equations and boundary conditions

The Navier-Stokes and the mass and energy equations in three-dimensional form were used to solve for the transient fluid dynamics with the coupled heat and mass transfer fields inside the finned tube adsorption bed system with silica gel/water or zeolite/water as the adsorbent/adsorbate working pairs. The mass balance describes the rate of adsorption or desorption within the adsorbent bed. The models were created in the COMSOL Multiphysics software package including the CFD, Heat Transfer and Chemical Reaction Engineering modules [31].

The governing equations of mass, momentum and energy conservation were solved by using the finite element method, based on the following assumptions:

- the finned tube adsorption bed operates under unsteady-state, non-equilibrium conditions;

- the surface porosity is considered to be equal to the total porosity;

- the volume fraction of the gas phase is assumed to be equal to the total porosity;

- the absorbent particles are assumed to have uniform size, shape and porosity;

- the adsorbate's water phase is assumed to be a liquid;

- the adsorbate's water vapour phase is assumed to be an ideal gas;

- the adsorbed phase is considered to be a liquid, while the gas phase is assumed to be an ideal gas;

- the working fluid is water at high velocity is assumed to be Newtonian, incompressible flow inside the tubes, resulting in a constant tube-surface temperature; the viscous dissipation and viscous work are neglected; there are no body forces;

- the work done by pressure changes, radiative heat transfer and viscous dissipation is neglected; and

- the wall thickness of the vacuum tube is assumed to be very thin and hence, its thermal resistance was neglected.

Therefore, the resulting governing equations can be stated as follows. For conciseness, the basic variables defined in the following equations can be found in [12–14, 24, 26, 28].

Conservation of mass:

$$\varepsilon \frac{\partial \rho_v}{\partial t} + (1 - \varepsilon)\rho_s \frac{\partial X}{\partial t} - D_m \Delta^2 \rho_v + \Delta(\boldsymbol{u}\rho_v) = 0 \qquad (1)$$

Conservation of momentum:
The momentum balance expresses the motion of the HTF within the tube.

$$\rho \frac{\partial \boldsymbol{u}}{\partial t} + \rho(\boldsymbol{u} \cdot \nabla)\boldsymbol{u} = \nabla \cdot \left[-pI + \mu \left(\nabla \boldsymbol{u} + (\nabla \boldsymbol{u})^2 \right) \right] \tag{2}$$

$$\rho \nabla \cdot (\boldsymbol{u}) = 0 \tag{3}$$

Conservation of energy:
The energy transfer within the system can be described with respect to the
three discrete domains involved: the HTF, the metal tube and fins, and the adsor-
bent. The adsorbent domain is assumed to be under local thermal equilibrium
between the adsorbed and vapour phase. Therefore, the equation has three addi-
tional terms to take into account for the change of temperature due to the water
vapour, water adsorbed and the heat of adsorption associated with the adsorption
process.
Heat transfer in the HTF:

$$\rho_f c_f \frac{\partial T_f}{\partial t} - k_f \Delta^2 T_f + \rho_f c_f v_f \Delta T_f = 0 \tag{4}$$

Heat transfer in the metal:

$$\rho_t c_t \frac{\partial T_t}{\partial t} - k_t \Delta^2 T_t = 0 \tag{5}$$

Heat transfer in the adsorbent:

$$\begin{gathered}
(1-\varepsilon)\rho_s c_s \frac{\partial T_s}{\partial t} - \varepsilon \rho_v c_{p,v} \frac{\partial T_s}{\partial t} + (1-\varepsilon)\rho_s X c_{p,l} \frac{\partial T_s}{\partial t} \\
-(1-\varepsilon)\rho_s |\Delta H| \frac{\partial X}{\partial t} - k_s \Delta^2 T_s + \rho_v c_{p,v} \boldsymbol{u} \Delta T_s = 0
\end{gathered} \tag{6}$$

The heat of adsorption (kJ/kg) changes linearly with the amount of water
adsorbed to the adsorbent [13]:

$$\Delta H = 2950 - 1400X \tag{7}$$

The velocity of the water vapour is calculated using Darcy's equation, which
defines the external mass transfer resistance in the water adsorption process.
Darcy's equation is valid in this condition since the adsorbent is porous and both the
velocity and the pressure are relatively low.
The 2D cylindrical and 3D Cartesian coordinate expressions are both
represented:

$$u = -\frac{\kappa}{\mu} \frac{\partial P}{\partial r}, v = -\frac{\kappa}{\mu} \frac{\partial P}{\partial z} \tag{8}$$

$$u = -\frac{\kappa}{\mu} \frac{\partial P}{\partial x}, v = -\frac{\kappa}{\mu} \frac{\partial P}{\partial y}, w = -\frac{\kappa}{\mu} \frac{\partial P}{\partial z} \tag{9}$$

The internal mass transfer resistance for the water adsorption process is defined
by means of a linear driving force expression as follows:

$$\frac{\partial X}{\partial t} = k_m (X_e - X) \tag{10}$$

where X represents the amount adsorbed and X_e is the equilibrium adsorption
capacity of the adsorbent-adsorbate pair under study, provided in Eqs. (13)–(18).

The temperature dependent mass transfer coefficient and diffusion coefficient are calculated as follows [25]:

$$k_m = \frac{15}{r_p^2} D_m \tag{11}$$

$$D_m = D_o \exp\left(-\frac{E_a}{RT_S}\right) \tag{12}$$

where D_o is reference diffusivity and r_p is the particle radius.

2.2.1 Kinetic expression for regular density (RD) silica gel

Regular density (RD) silica gel is the most widespread type of silica gel and is obtainable from any supplier that retails silica gel. Because of its capacity for high moisture uptake in the low RH (relative humidity) range, it is a very effective desiccant.

The equilibrium adsorption capacity characterises the theoretical maximum capacity that the adsorbent bed can adsorb for a given pressure and temperature [32].

For RD silica gel, the following pressure dependent isotherm is used as follows:

$$X_e = a \left(\frac{P}{P_{sat}}\right)^b \tag{13}$$

The values of a and b are temperatures dependent are provided in the next section, **Table 1** and given as follows [33]:

$$a = a_0 + a_1 T_s + a_2 T_s^2 + a_3 T_s^3 \tag{14}$$

$$b = b_0 + b_1 T_s + b_2 T_s^2 + b_3 T_s^3 \tag{15}$$

The saturated water pressure (kPa) for the adsorbate is provided by Antoine's equation [34].

$$P_{sat} = 0.1333 \cdot 10^{8.07131 - \frac{1730.63}{T_s - 39.724}} \tag{16}$$

2.2.2 Kinetic expression for zeolite 13X

The equilibrium adsorption capacity for zeolite 13X is determined with the following Dubinin-Astakhov (D-A) equation as the adsorption isotherm where the values of B and n are constants [35]:

$$X_e = X_o \exp\left[-B\left(\frac{T_s}{T_{sat}} - 1\right)^n\right] \tag{17}$$

The saturated water temperature (K) for the adsorbate is given by Antoine's equation [34] as follows:

$$T_{sat} = 39.724 + \frac{1730.63}{8.07131 - \log 10\left(7.500638 \cdot 10^{-3} \cdot P\right)} \tag{18}$$

Assuming symmetry conditions, the boundary conditions in a view of the 2D axisymmetric finned adsorbent, used in this work are depicted **Figure 3**. At the upstream or inlet boundary, Dirichlet boundary conditions, uniform flow with

Category	Description	Variable	Unit	Validation zeolite 13X/water	Base case silica gel/water
Temperature pressure	Hot temperature	T_{hot}	K	473	338
	Cold temperature	T_{cold}	K	313	298
	Condenser pressure	P_c	kPa	4.247	4.246
	Evaporator pressure	P_e	kPa	n/a	1.228
	Adsorption initial concentration	X_{a0}	kg/kg	—	0.024
	Desorption initial concentration	X_{d0}	kg/kg	—	0.72
Geometry	Bed thickness	l_{bed}	mm	13	12
	Fin distance	d	mm	10	15
	Tube thickness (copper)	b	mm	1	1
	Adsorbent particle diameter	d_p	mm	1.25	3
	Absorber length	L	mm	500	600
	Tube radius	r_t	mm	13	13
	Tube thickness	b_t	mm	1	1
	Void fraction	ε	—	0.635	0.635
	Permeability	κ	m^2	3.04e-7	3.4e−9
Mass	Reference diffusivity	D_o	m^2/s	5.8e-9	2.54e−4
	Activation energy of surface diffusion	E_a	J/mole	1.0e5	3.36e4
	Fluid density	ρ_f	kg/m^3	914	f(T)
	Absorbent density	ρ_s	kg/m^3	1000	670
	Tube density	ρ_t	kg/m^3	8700	8700
	Dynamic viscosity	μ	kg/m s	1.0e-5	1.5e−5
Thermal properties	Fluid velocity	v	m/s	0.001	0.001
	Thermal conductivity of bed	k_s	W/m K	1	0.3
	Thermal conductivity of fluid	k_f	W/m K	0.155	f(T)
	Thermal conductivity of tube	k_t	W/m K	400	400
	Convective heat transfer coefficient: tube and adsorbent	h_o	W/m^2 K	100	100
	Convective heat transfer coefficient: tube and fluid	h_i	W/m^2 K	100,000	100,000
	Specific heat of fluid	c_f	J/kg K	1930	f(T)
	Specific heat of particle liquid	c_{pl}	J/kg K	4180	4180
	Specific heat of particle vapour	c_{pv}	J/kg K	1880	1880
	Specific heat of adsorbent solid	c_s	J/kg K	837	f(T)
	Specific heat of tube	c_t	J/kg K	385	f(T)
Kinetics	Water adsorbed reference	X_o	kg$_w$/kg$_s$	0.261	—
	D-A constant	B	—	5.36	—
	D-A constant	n	—	1.73	—

Category	Description	Variable	Unit	Validation zeolite 13X/water	Base case silica gel/water
	Kinetic constant	a_0	—	—	−6.5314
	Kinetic constant	a_1	—	—	0.072452
	Kinetic constant	a_2	—	—	−0.00023951
	Kinetic constant	a_3	—	—	2.5493e−7
	Kinetic constant	b_0	—	—	−15.587
	Kinetic constant	b_1	—	—	0.15915
	Kinetic constant	b_2	—	—	−0.00050612
	Kinetic constant	b_3	—	—	5.329e−7
Misc.	Universal gas constant	R	J/mole K	8.314	8.314
	Ideal gas constant for water vapour	R_v	J/kg K	461.5	461.5

Table 1.
Parameter settings for the validation and parametric studies.
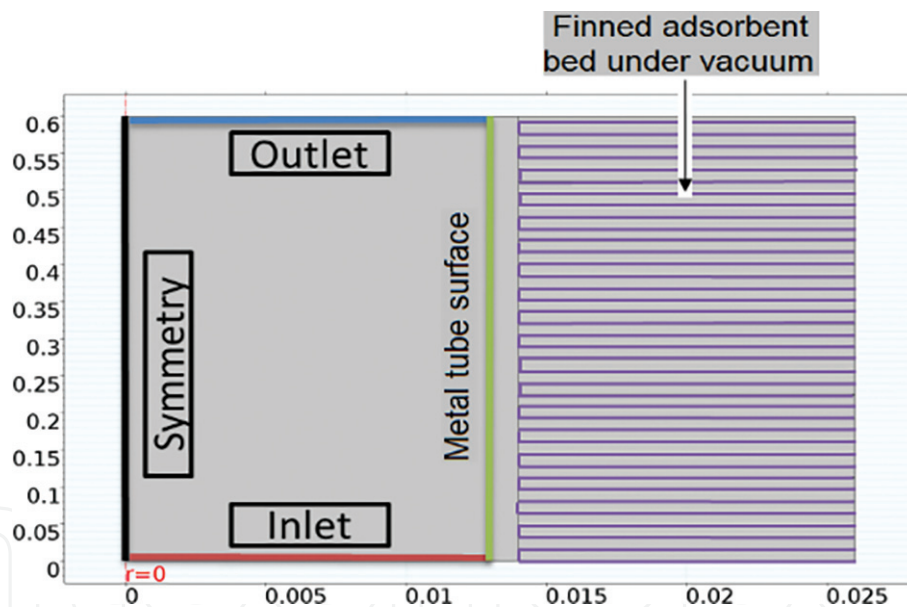
Figure 3.
View of the 2D axisymmetric finned tube adsorber: computational domain with boundary conditions.

constant velocity and constant temperature are assumed. At the downstream end of the computational domain or outlet, the Neumann boundary condition is used, i.e. stream wise gradients for all the variables are set to zero. No-slip boundary condition is used at the adsorbent fin surfaces. These surfaces are assumed to be solid walls with no slip wall boundary condition; the velocity of the fluid at the wall is zero and constant wall temperature is presumed. This sweeping statement relates to isothermal wall boundary condition. The fins and tube are presumed to be made of copper. As copper is a rather high thermal conductivity material, constant wall temperature boundary condition can be confidently supposed throughout the shells. In the right side of the figure, is shown the adsorbent bed under vacuum, where there is zero flux for mass transfer.

For energy transfer, symmetry, inlet and outlet of the metal tube, have the same definitions as in the momentum transfer physics. However, the metal tube surface with the fins shown in green and purple lines, define the heat transfer between the three domains. The convective heat transfer boundary conditions between the heat transfer fluid, metal tube and the adsorbent are defined as follows:

HTF to metal tube:

$$q_i = h_i\left(T_t - T_f\right) \tag{19}$$

where h_i is the convective heat transfer coefficient between tube and fluid.
Metal tube to adsorbent:

$$q_o = h_o\left(T_s - T_t\right) \tag{20}$$

where h_0 is the convective heat transfer coefficient between tube and adsorbent.

2.3 Numerical procedure

The governing equations of mass, momentum and energy conservation are solved by using the finite element method, based on the assumptions listed in Section 2.2. The governing equations are discretised on the computational domain, linearised in an implicit manner and solved by the finite element method using a pressure-based coupled solver (PBCS). This latter solves pressure and momentum
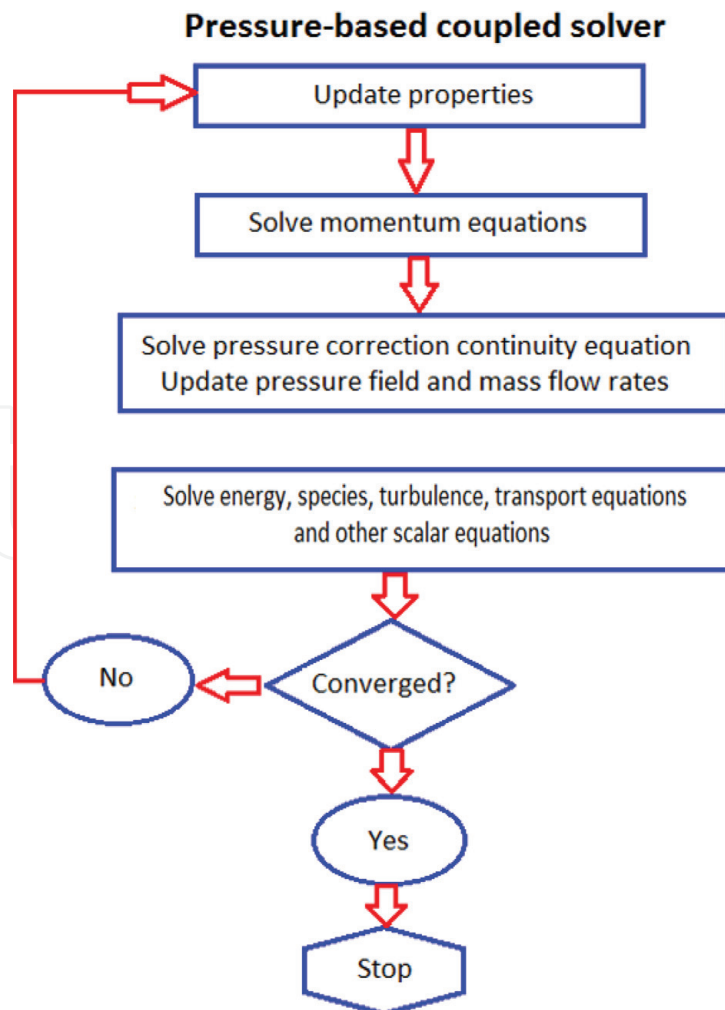
Figure 4.
Overview of the pressure-based coupled solver algorithm.

simultaneously. **Figure 4** represents an overview of the PBCS algorithm. SIMPLEC (Semi-Implicit Method for Pressure Linked Equations-Consistent) algorithm is applied for the pressure-velocity coupling; the second order upwind discretisation scheme is used for the convection terms and each governing equation is solved using QUICK (Quadratic Upwind Interpolation) scheme [36].

It is required to carry out independency verification of the grid system before CFD computation. The mesh independence study is examined by utilising three different mesh sizes (normal, fine and finest meshes) of 23,083, 35,305, and 84,992 for the finned tube adsorption cooling bed are adopted for computation for the baseline case. The relative error compared to the fine mesh, in the average bed temperature and the total water adsorbed as a function of time, are 2.85 and 1.84%, and 0.13 and 0.07%, respectively, before settling to a fine mesh for the geometry of the computational adsorption cooling bed cases. Computations were then run for a geometry comprising about 35,305 meshes, which was considered satisfactory in terms of accuracy and efficiency.

Furthermore, the solution is iterated until convergence is achieved, that is, residual for each equation achieves values less than 10^{-6}, and variations in energy, mass and temperature, respectively become negligible. A workstation with 2 (R) Xeon processors and a 2 core 2.4 GHz CPU with an installed memory of 32 GB (RAM), which took between 4 and 8 hours of CPU time depending on the computation case, was utilised to execute the necessary task.

3. Model validation

Experimental data of a finned tube adsorption bed with zeolite/water (adsorbent/adsorbate) as the working pair, zeolite as the adsorbent material by Çağlar et al. [28] have been used to validate the CFD model in the present study. The finned tube heat exchanger geometry was modified to have the identical geometric dimensions and operating conditions as found in [27]. **Table 1** shows the parameter settings associated with the experimental operation with particular settings associated with the experimental tests for t, k, v, l_{bed} and r shown in **Figure 5**. In **Figure 4**
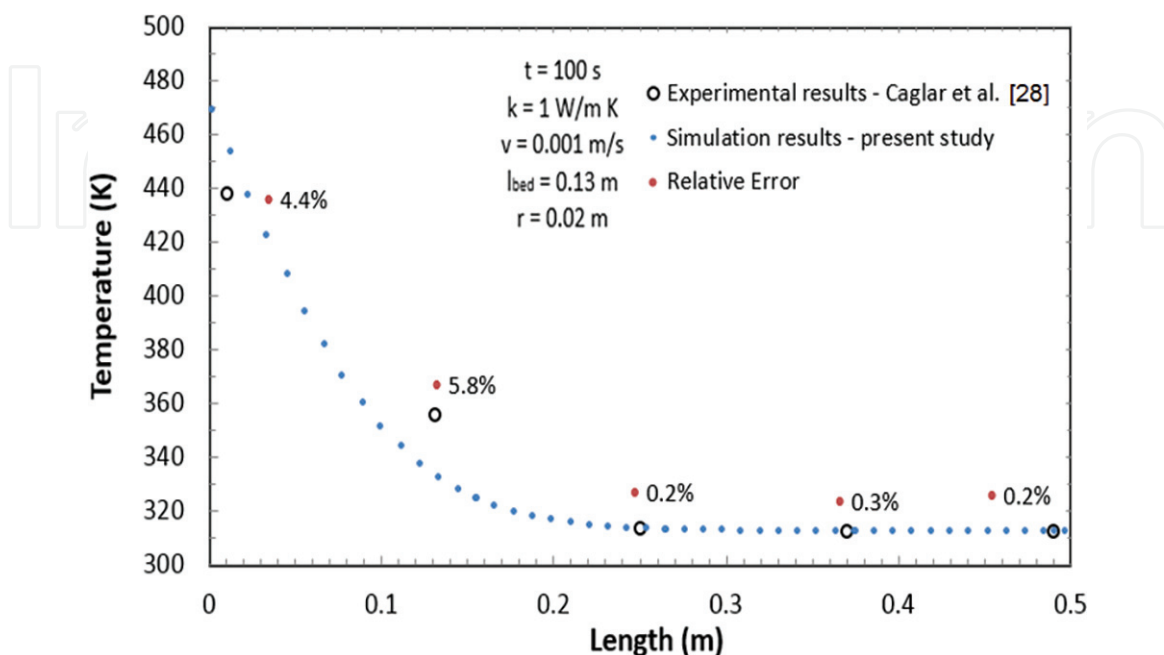

Figure 5.
Comparison of simulation results with experimental results of Çağlar et al. [28] in finned tube adsorption cooling system using zeolite/water for validation study.

shows the results of the simulated temperature profile in COMSOL Multiphysics along r = 0.02 m of the unit. It can be seen that the experimental data for the desorption mode compared to the CFD simulation results provide good agreement between the each other with deviation of no more than 5.8%. The difference between the experimental and numerical results is higher at the inlet of the unit. This may be due to the experimental uncertainties due to the temperature measurement errors because of lower heat transfer resulted from flow maldistribution or various losses. However, the observed uncertainties are well within the uncertainties of sensor measurements. This CFD model of the adsorption cooling system was therefore utilised for further transient analysis with supporting reliability of the computation.

4. Results and discussion

The selected adsorption chiller applied a finned tube geometry with a silica gel/water working pair. A base line case on desorption mode is initially simulated and studied to determine the intrinsic behaviour of the system. The parameter values for the base case and for the parametric study are presented in **Table 1**.

4.1 Base case

Figure 6 presents a 3D qualitative assessment of the pressure, temperature and water desorption distributions at operation times of 200, 600 and 1200 s. The temperature profile captures the heat transfer characteristics of the system throughout the entire system while the pressure and adsorbed water only capture phenomena in the adsorbent bed. Desorption is the mode of operation highlighted in this study. The HTF inlet temperature is 338 K while the bed temperature is 298 K. The HTF enters the tube at z = 0 and exits at z = 0.6 m. A white set of arrows
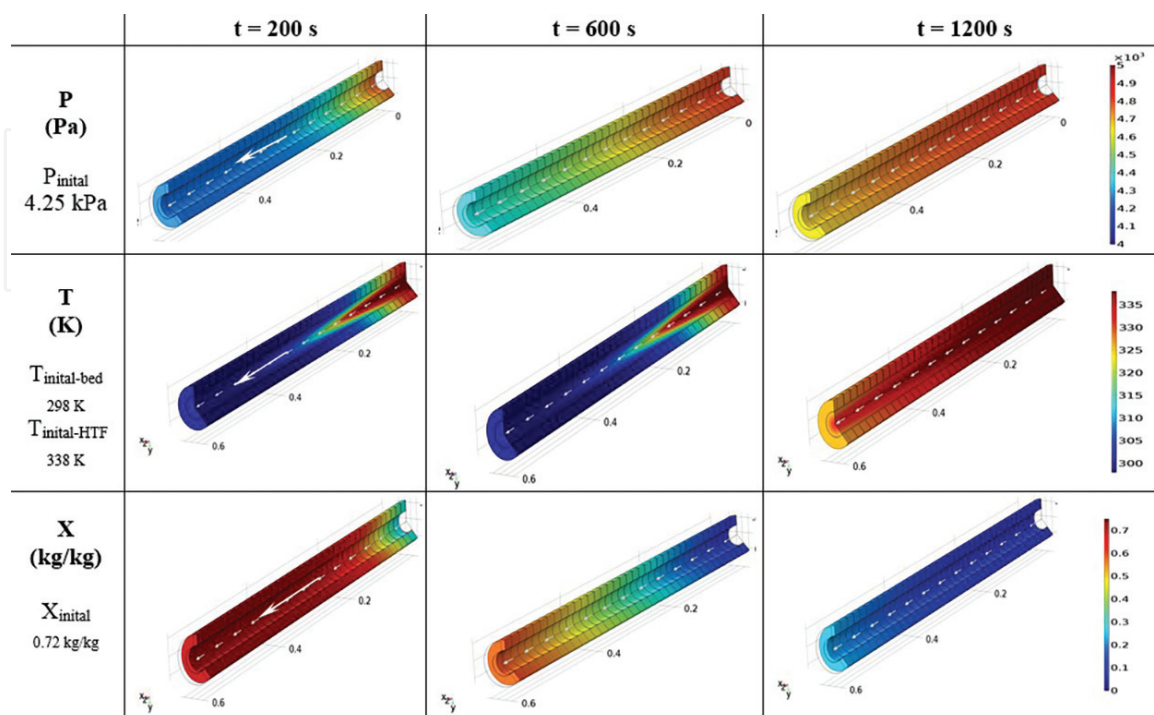

Figure 6.
Pressure, temperature and adsorbed water distributions at t = 200, 600 and 1200 s of the 3D geometry for the baseline case under desorption mode.

show the direction of the fluid flow. The kinetics of the adsorbed water is slow enough that there exists a time delay between reaching the thermodynamic temperature and establishing the equilibrium. The adsorbent is fully saturated after 2000 s, but this is not illustrated on the figure for brevity. For desorption the initial pressure of the system increases to 4.246 kPa and the initial adsorbed water begins at 0.72 kg/kg and reaches 0.08 kg/kg upon completion. The pressure of the system closely follows the behaviour of the temperature profile and affects the equilibrium water adsorption.

Figure 7 presents a 2D qualitative assessment of the pressure, temperature and desorbed water distributions. The same layout and results are chosen to be displayed as in **Figure 6** for an alternative, but more insightful, assessment of the simulation results. From this visual perspective, the profiles for all simulated measures may be better compared in the parametric study.

4.2 Parametric study

A parametric study applying the developed transient CFD coupled with heat and mass transfer model, was conducted in an effort to predict the influence of various parameters on the design and performance of an adsorption cooling system during the desorption process. The effect of these parameters on the governing independent parameters influencing the fluid flow, the heat and mass transfer on the adsorber performance, are the geometrical, particle size, physical-chemical, thermodynamic and thermal property parameters of the adsorber. The parameters investigated in this study are the adsorbent bed thickness (l_{bed}), the heat exchanger tube thickness (b), the HTF velocity (v), and the adsorbent particle diameter (d_p).
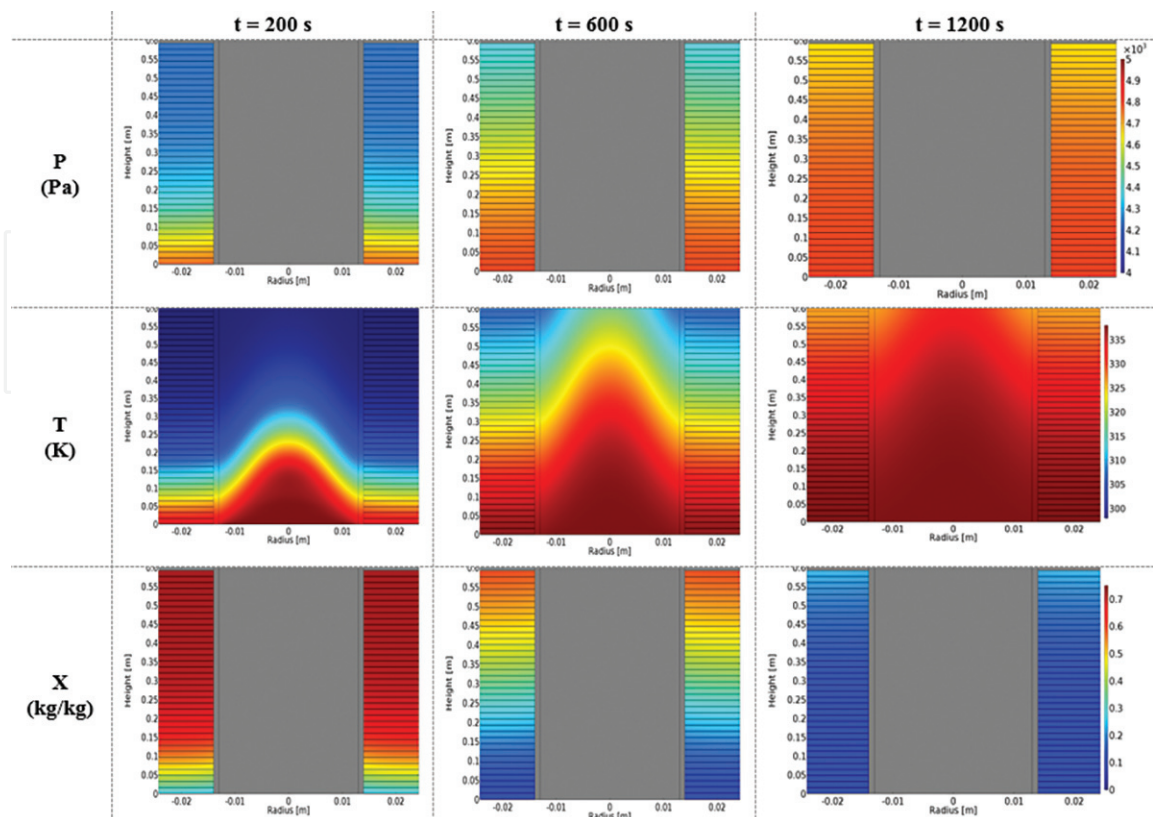

Figure 7.
Pressure, temperature and adsorbed water distributions at t = 200, 600 and 1200 s of the 2D geometry for the baseline case under desorption mode.

Case description			Geometry		Fluid flow and particle size properties	
Case	Case no.	Case description	Bed thickness	Tube thickness	HTF velocity	Adsorbent particle diameter
			l_{bed} (mm)	b (mm)	v (m/s)	d_p (mm)
1	1	Base	12	1	0.001	3
2	2	Bed thickness	30	1	0.001	3
	3		45			
3	4	Tube thickness	12	1.5	0.001	3
	5			2		
4	6	Fluid velocity	12	1	0.005	3
	7				0.015	
5	8	Adsorbent particle diameter	12	1	0.001	2
	9					5

Table 2.
Summary of the simulation matrix with the input data of the adsorption cooling system.

The basic aim of the analysis is to better understand the optimum design of the adsorption cooling system with heat exchanger configurations using CFD approach and, thereby, learn how to successfully maximise the overall heat and mass transfer performance of the system such as temperature and desorption rates whilst minimising the pressure drop.

Table 2 depicts the four-parameter settings, which were selected in the study. Eight cases were investigated.

4.2.1 Effect of adsorbent bed thickness (l_{bed})

The effect of adsorbent bed thickness on the dependent variables pressure, temperature and amount of water adsorbed within the adsorption cooling system is investigated for adsorbent bed thicknesses of 12 (baseline case), 30 and 45 mm. **Figure 8** presents the effect of bed thickness on simulated transient average bed pressure, average bed temperature and adsorption of water profiles. **Figure 9** shows the simulated temperature and water adsorbed distributions at t = 600 s.

The results reveals that the thickness of adsorbent bed has a substantial effect on the desorption performance. As the bed thickness increases, the bed temperature takes more time to increase. Therefore, the rate of the pressure drop is lower and the water adsorption takes a greater extent of time. The pressure, temperature and the amount of water adsorbed distributions inside the bed reaches equilibrium after about 1500, 2500 and 3000 s for bed thicknesses of 12, 30 and 45 mm, respectively. The desorption bed produced decreased average pressure values of 0.8 and 1.6%, for adsorption bed thicknesses of 30 and 40 mm relative to the baseline case having a bed thickness of 12 mm, respectively. Alternatively, under the same conditions, the desorption bed produced the same amounts of decreased average temperature and decreased adsorbed water values of 15.3 and 35.0%, respectively.

As adsorbent bed thickness increases, more adsorbent is used, external mass transfer resistances increase with increasing mass of adsorbent. Thus, more heat is expected to be required to increase the temperature of the entire unit; the thermal resistances across the adsorbent bed are substantially increased. Fin temperature is reduced and cannot generate a sufficient heat transfer since the contact resistances between fins and adsorbent material increase. This causes reduced mass transfer, smaller amounts of adsorption capacities and increased cycle times. This same
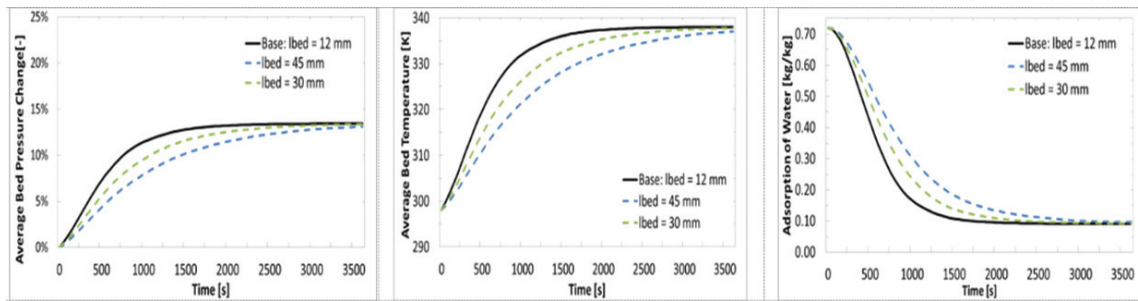
Figure 8.
Effect of bed thickness (l_{bed}) on desorption 1D profile as a function of time for average bed pressure drop, average bed temperature and adsorption of water.
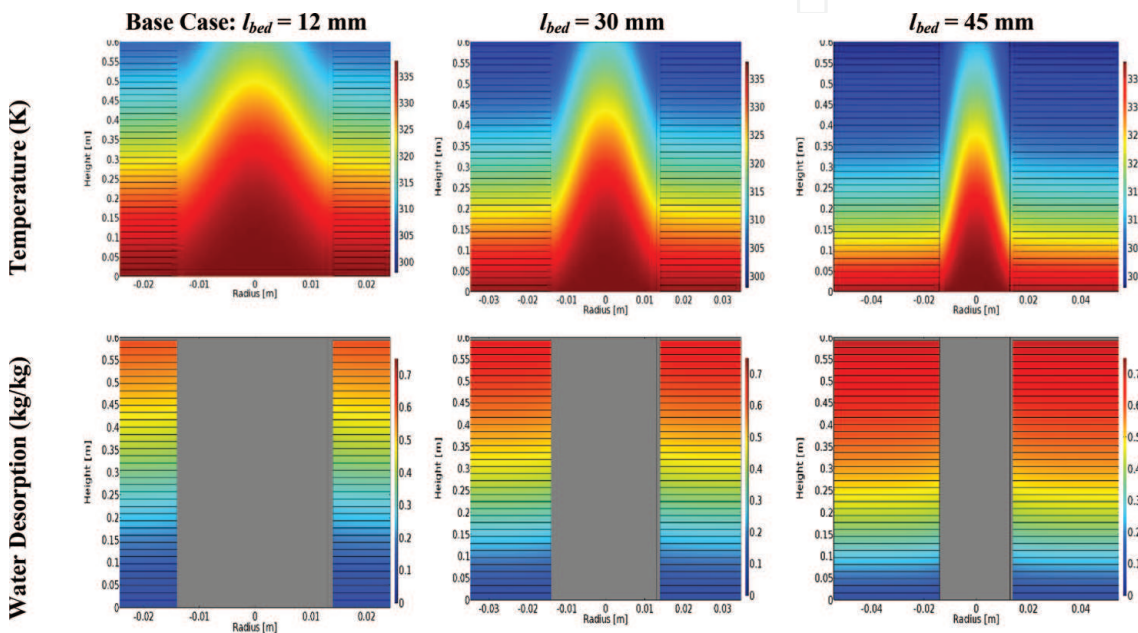

Figure 9.
Effect of bed thickness (l_{bed}) on desorption 2D temperature and adsorbed water distributions at t = 600 s.

outcome has been documented by previous researches in heat exchangers in general. Heat transfer in the radial direction is improved by reducing the adsorbent bed thickness. For design considerations, a reduced adsorbent bed thickness will produce a reduced cycle time and an enhanced specific cooling power. Increasing bed thickness has then an adverse effect on the heat transfer within the bed. There is a trade-off to consider; decreasing bed thickness, results in an improvement in the heat transfer across the adsorbent bed at the expense of a reduction in the mass of adsorbent and hence, of the adsorption capacity.

4.2.2 Effect of tube thickness (b)

The effect of tube thickness on the dependent variables pressure, temperature and amount of water adsorbed within the adsorption cooling system is examined for tube thickness of 1 (baseline case), 1.5 and 2 mm. **Figure 10** shows the effects of tube thickness on simulated transient average bed pressure, average bed temperature and adsorption of water profiles. **Figure 11** presents the simulated temperature and water adsorbed distributions at t = 600 s.
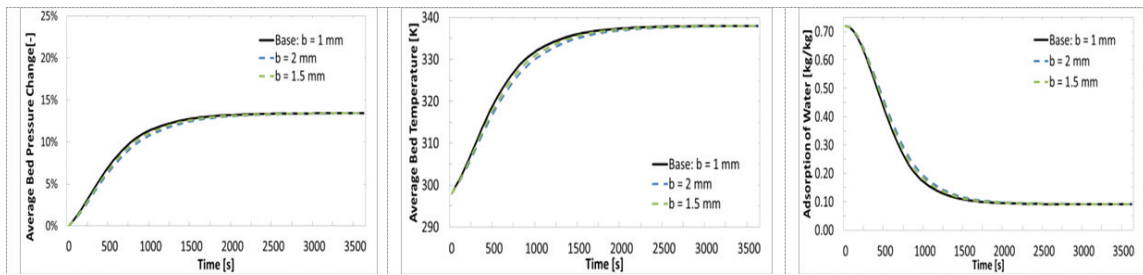
Figure 10.
Effect of tube thickness (b) on desorption 1D profiles as a function of time for average bed pressure drop,
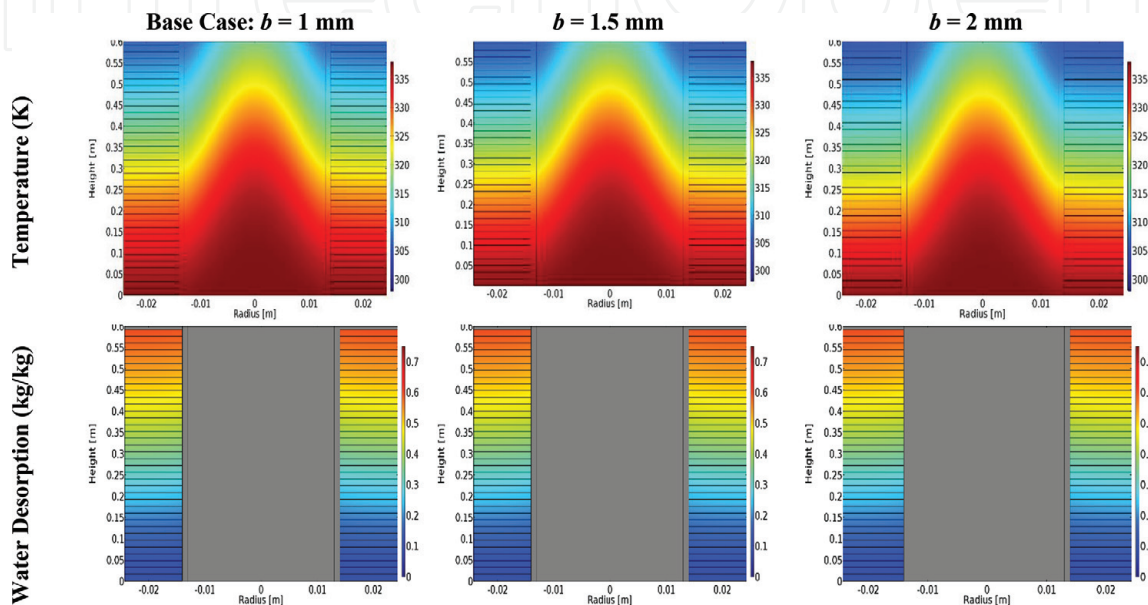*average bed temperature and adsorption of water.*

Figure 11.
Effect of tube thickness (b) on desorption 2D temperature and adsorbed water distributions at t = 600 s.

The data in the figures disclose that as the tube thickness increases, neither the bed temperature, pressure or water adsorption shows any significant variance from the baseline case. It is expected that as tube thickness increases, a greater amount of heat should be transferred to the adsorbent bed, and thus should have a positive impact on the overall performance. However, the limited process is controlled by the heat and mass transfer phenomena in the adsorption cooling system. Heat and mass transfer coefficients of the bed are quite small due to low conductivity of adsorbent particles, and high contact resistance between particles and metal tubes/fins. Therefore, the performance of the adsorbent bed is affected unfavourably by the heat and mass transfer constraints inside the bed, with reduced thermal conductivity of the solid adsorbent, and internal (intra-particle) and external (inter-particle) mass transfer resistances.

4.2.3 Effect of HTF velocity (v)

The effect of HTF velocity on the dependent variables pressure, temperature and amount of water adsorbed within the adsorption cooling system is evaluated for velocity of 0.001 (baseline case), 0.005 and 0.015 m/s. **Figure 12** shows the effects of HTF velocity on simulated transient average bed pressure, average bed temperature and adsorption of water profiles. **Figure 13** presents the simulated temperature and water adsorbed distributions at t = 600 s.
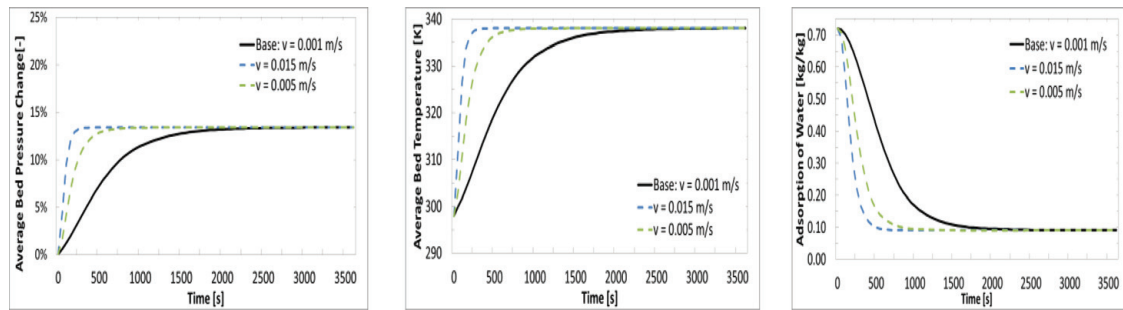
Figure 12.
Effect of HTF velocity (v) on desorption 1D profiles as a function of time for average bed pressure drop, average bed temperature and adsorption of water.
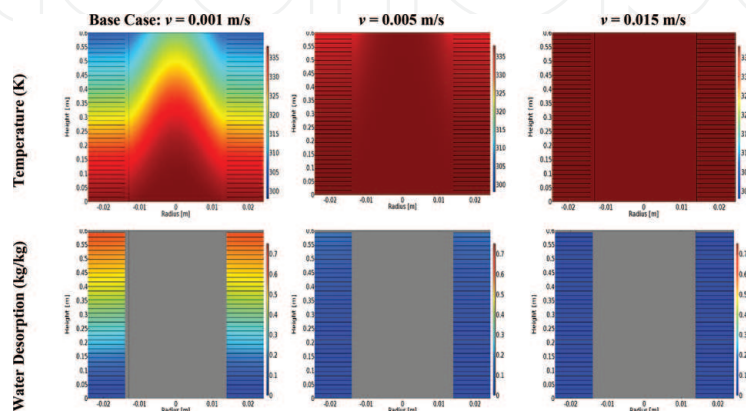

Figure 13.
Effect of HTF velocity on desorption 2D temperature and adsorption of water distributions at t = 600 s.

The results reveal that as the HTF velocity increases, the bed temperature and pressure response increase substantially, as well as the water desorbed. With an increase of HTF velocity from 0.001 to 0.005 m/s the water desorption response almost decreases an upper threshold. Alike, for the fluid flow and thermal properties, as fluid velocity of the tube increases, the temperature profile evolution should rise. The desorption bed produced increased average pressure and temperature values of 1.3 and 1.7% for HTF velocity of 0.055 and 0.015 relative to the baseline case having a HTF velocity of 0.001 m/s, respectively. On the other hand, under the same conditions, the desorption bed produced decreased average adsorbed water values of 18 and 21%, respectively. The adsorbent bed reached a steady state uniform temperature profile at the cycle maximum temperature of 338 K at 500, 700 and 1500 s, respectively. The cycle time increases with the decrease of the HTF velocity in the heat exchanger. An optimal velocity value corresponding to maximum overall performance of the adsorption cooling system, such as a high COP and specific cooling power would be in the range between 0.005 and 0.015 m/s. The HTF velocity should be well selected in order to obtain a good heat transfer efficiency, but also a positive effect on the mass transfer inside the adsorbent bed and on the overall system performance. A too slow HTF will increase cycle time and decrease specific cooling power. A faster velocity will reduce thermal gradient, but will need more pumping energy.

4.2.4 Effect of adsorbent particle diameter (d_p)

The effect of adsorbent particle diameter on the dependent variables pressure, temperature and amount of water adsorbed within the adsorption cooling system is assessed for particle diameter of 2, 3 (baseline case) and 5 mm. **Figure 14** presents
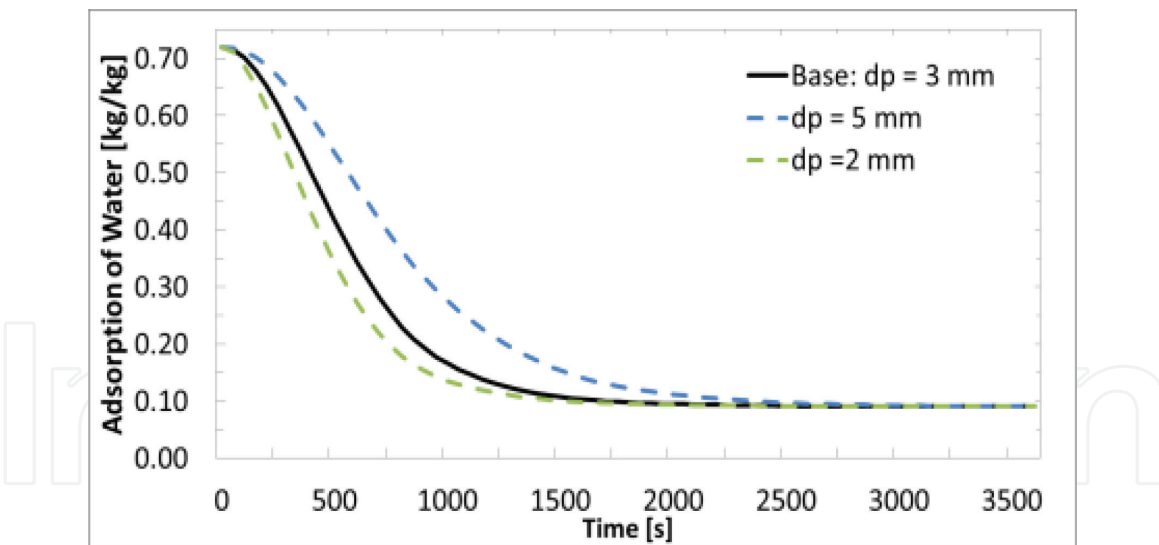
Figure 14.
Effect of particle diameter (d_p) on desorption 1D profiles as a function of time for adsorption of water.
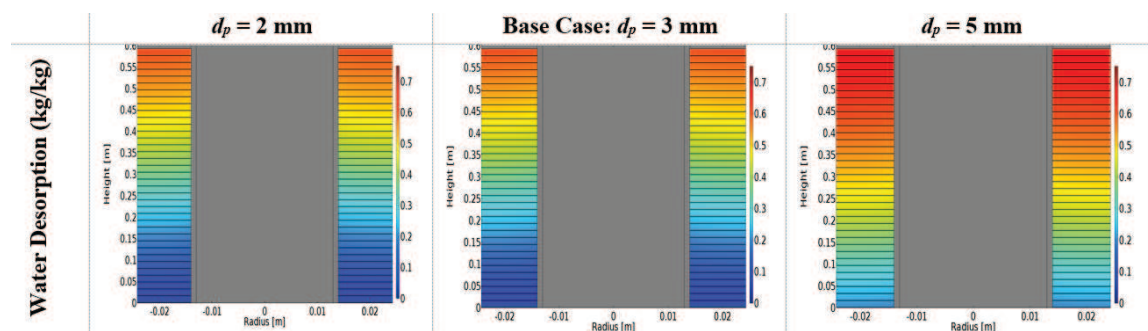

Figure 15.
Effect of particle diameter (d_p) on desorption 2D adsorbed water distributions at t = 600 s.

the effects of particle diameter on simulated transient adsorption of water profile. **Figure 15** shows the water adsorbed distributions at t = 600 s. The temperature and pressure profiles are not shown because of limited space.

The desorption bed produced decreased/increased average temperature and pressure values of about 1.6% for adsorbent particle diameter of 2 mm and 5 mm relative to the baseline case having a particle diameter of 3 mm, respectively. Alternatively, the desorption bed produced decreased average adsorbed water value of 6% for adsorbent particle diameter of 2 mm, and increased value of 22% for adsorbent particle diameter of 5 mm, relative to the baseline case having a particle diameter of 3 mm. The adsorbent bed achieved a steady state uniform temperature profile at the cycle maximum temperature of 338 K at 1000, 1500 and 2000 s, respectively. The smaller the particle diameter the faster the water adsorption response. The kinetics is directly dependent upon the particle packing as seen by the kinetic expressions in Section 2. As the adsorbent particle diameter decreases, the specific area of adsorbent increases, the internal mass transfer resistances decrease. Therefore, the bed temperature, the pressure and the desorption rate increase. The particle diameter should be kept as smaller as possible.

5. Conclusions

In this work, a transient CFD coupled with heat and mass transfer model has been created for a solar adsorption cooling system. Transient simulations have been

carried out to investigate the influence of several design and operating parameters during the desorption process. Silica gel and zeolite 13X are both investigated as possible adsorbents, though the study incorporated the working pair silica gel/water given the lower working temperature range required for operation which makes it more suitable for residential cooling applications powered by solar heat. Flow behaviour, heat and mass transfer performances have been analysed in detail. The CFD model was validated against the experimental data using zeolite 13X/water pair available in the literature. Good agreement with experimental results was obtained, which demonstrates the effectiveness of the model. Therefore, the CFD model was utilised in the present study with confidence that it can predict the pressure, temperature and water adsorption of the system accurately.

The key parameters considered in this work were geometrical and operating factors such as bed thickness (l_{bed}), heat exchanger tube thickness (b) and HTF velocity (v), and adsorbent particle diameter (d_p). The results have not only confirmed some observations reported in earlier researches, but also provided an envelope for the optimum design parameters when the operating conditions and geometrical factors were varied for performance enhancement. In order of highest impact on the system, the parameters are listed as follows: $v > d_p > l_{bed} > b$. The results disclosed that from the four parameters; only the first three stated are the most influential factors of performance and significantly change the cycle time. In the design phase, the most important geometric parameter to consider is the bed thickness. As the bed thickness increases, the amount of water adsorbed increases but so does the cycle time. While selecting the adsorbent material, a smaller particle diameter is desired to minimise the cycle time. A lower threshold of 2 mm was identified. During operation, the fluid velocity should be operated at a higher velocity to minimise the cycle time. A upper threshold of 0.005 m/s was identified.

It is concluded that the present modelling approach provides a useful means of identifying significant features, which influence the levels of the pressure drops, temperature and water adsorption from adsorption cooling systems and for assessing the performance characteristic of proposed adsorption chiller configurations. Moreover, the coupled CFD with heat and mass transfer model is a useful tool to simulate and optimise adsorption cooling systems and detect the parameters in the adsorber that are responsible for excessive pressure drops and low performance levels. The effort to alleviate these problems can be directly evaluated. In addition, the influence of any modification that is made to help improve performance characteristics on other operating or geometrical parameters is easily evaluated.

As a final point, this work should lead to accurate design and optimisation of solar/heat-driven adsorption cooling systems in terms of better control of the heat and mass transfer levels over the entire adsorption/desorption operating range and improved overall system performance.

Acknowledgements

Conflict of interest

The authors declare no conflict of interest.

Nomenclature

a	kinetic constant
b	kinetic constant
b	tube thickness, m
b_t	tube thickness, m
C	specific heat capacity, J/kg K
COP	coefficient of performance
d	fin distance, m
D_o	reference diffusivity, m^2/s
D_m	molecular diffusivity, m^2/s
D-A	Dubinin-Astakhov
d_p	adsorbent particle diameter, m
E_a	activation energy of surface diffusion, J/mol
h_i	convective heat transfer coefficient: tube and fluid, W/m^2 K
h_o	convective heat transfer coefficient: tube and adsorbent, W/m^2 K
ΔH	heat of adsorption, kJ/kg
I	identity tensor
k	thermal conductivity, W/m K
k_m	mass transfer coefficient, 1/s
L	adsorbent bed total length, m
l_{bed}	bed thickness, m
P	pressure, kPa
r_p	particle radius
R	universal gas constant, J/mol K
RD	regular density
R_v	ideal gas constant for water vapour, J/kg K
SPC	specific cooling power, W/kg
T	temperature, K
$\boldsymbol{u}$	velocity vector, m/s
v	fluid velocity, m/s
X	adsorption of water, kg_w/kg_s

Greek letters

Δ	gradient operator
Δ^2	Laplacian operator
ε	void fraction
κ	permeability, m^2
μ	dynamic viscosity, kg/m s
ρ	density, kg/m^3

Subscripts

0	initial condition
a	adsorption
b	adsorbent bed
c	condenser
cold	low temperature setting
d	desorption
e	equilibrium or evaporator

f	fluid
hot	high temperature setting
pl	particle liquid
pv	particle vapour
s	solid adsorbent
v	vapour
t	tube

Author details

Wahiba Yaïci* and Evgueniy Entchev
CanmetENERGY Research Centre, Natural Resources Canada, Ottawa, Ontario,
Canada

*Address all correspondence to: wahiba.yaici@canada.ca

IntechOpen

References

[1] Saha BB, Akisawa A, Kashiwagi T. Solar/waste heat driven two-stage adsorption chiller: The prototype. Renewable Energy. 2001;**23**:93-101. DOI: 10.1016/S0960-1481(00)00107-5

[2] Tso CY, Chao CYH. Activated carbon, silica-gel and calcium chloride composite adsorbents for energy efficient solar adsorption cooling and dehumidification systems. International Journal of Refrigeration. 2012;**35**: 1626-1638. DOI: 10.1016/j. ijrefrig.2012.05.007

[3] Sah RP, Choudhury B, Das RK. A review on adsorption cooling systems with silica gel and carbon as adsorbents. Renewable and Sustainable Energy Reviews. 2015;**45**:123-134. DOI: 10.1016/j.rser.2015.01.039

[4] Meunier F. Solid sorption: An alternative to CFCs. Heat Recovery CHP. 1993;**13**:289-295. DOI: 10.1016/ 0890-4332(93)90051-V

[5] Meunier F. Solid sorption heat powered cycles for cooling and heat pumping applications. Applied Thermal Engineering. 1998;**18**:715-729. DOI: 10.1016/S1359-4311(97)00122-1

[6] Teng Y, Wang RZ, Wu JY. Study of the fundamentals of adsorption systems. Applied Thermal Engineering. 1997;**17**: 327-338. DOI: 10.1016/S1359-4311(96) 00039-7

[7] Pons M, Meunier F, Cacciola G, Critoph R, Groll M, Puigjaner L, et al. Thermodynamic based comparison of sorption systems for cooling and heat pumping. International Journal of Refrigeration. 1999;**22**:5-17. DOI: S0140-7007(98)00048-6

[8] Hamamoto Y, Alam KC, Saha BB, Koyama S, Akisawa A, Kashiwagi T. Study on adsorption refrigeration cycle utilizing activated carbon fibers. Part 2:

Cycle performance evaluation. International Journal of Refrigeration. 2006;**29**:315-327. DOI: 10.1016/j. ijrefrig.2005.06.001

[9] Shmroukh AN, Ali AHH, Ookawara S. Adsorption working pairs for adsorption cooling chillers: A review based on adsorption capacity and environmental impact. Renewable and Sustainable Energy Reviews. 2015;**50**: 445-456. DOI: 10.1016/j. rser.2015.05.035

[10] Kim AS, Lee HS, Moon DS, Kim HJ. Performance control modeling on adsorption desalination using initial time lag (ITL) of individual beds. Desalination. 2016;**369**:1-16. DOI: 10.1016/j.desal.2016.05.004

[11] Zhang LZ, Wang L. Effects of coupled heat and mass transfers in adsorbent on the performance of a waste heat adsorption cooling unit. Applied Thermal Engineering. 1999;**19**: 195-215. DOI: 1359-4311/99

[12] Zhang LZ. A three-dimensional non-equilibrium model for an intermittent adsorption cooling system. Solar Energy. 2000;**69**:27-35. DOI: 0038-092X/00

[13] Solmuş İ, Rees DAS, Yamalı C, Baker D. A two-energy equation model for dynamic heat and mass transfer in an adsorbent bed using silica gel/water pair. International Journal of Heat and Mass Transfer. 2012;**55**:5275-5288. DOI: 10.1016/j.ijrefrig.2011.12.006

[14] Yong L, Sumathy K. Review of mathematical investigation on the closed adsorption heat pump and cooling systems. Renewable and Sustainable Energy Reviews. 2002;**6**:305-338. DOI: 10.1016/S1364-0321(02)00010-2

[15] Teng WS, Leong KC, Chakraborty A. Revisiting adsorption cooling cycle

from mathematical modelling to system development. Renewable and Sustainable Energy Reviews. 2016;**63**: 315-332. DOI: 10.1016/j.rser.2016.05.059

[16] Sakoda A, Suzuki M. Fundamental study on solar powered adsorption cooling system. Journal of Chemical Engineering of Japan. 1984;**17**:52-57. DOI: 10.1252/jcej.17.52

[17] Cho SH, Kim JN. Modeling of a silica gel/water adsorption cooling system. Energy. 1992;**17**:829-839. DOI: 10.1016/ 0360-5442(92)90101-5

[18] Cacciola G, Restuccia G. Reversible heat pump: A thermodynamic model. International Journal of Refrigeration. 1995;**18**:100-106. DOI: 10.1016/ 0140-7007(94)00005-I0007/95/ 0140-7

[19] Guilleminot JJ, Meunier F, Pakleza J. Heat and mass transfer in a non-isothermal fixed bed solid adsorbent external reactor: A uniform pressure–non uniform temperature case. International Journal of Heat and Mass Transfer. 1987;**30**:1595-1606. DOI: 10.1016/0017-9310(87)90304-8

[20] Aittomaki A, Harkonen M. Modelling of zeolite/methanol adsorption heat pump process. Heat Recovery Systems CHP. 1988;**8**:475-482. DOI: 10.1016/0890-4332(88)90053-1

[21] Shelton SV, Wepfer WJ, Miles DJ. External fluid heating of a porous bed. Chemical Engineering Communications. 1988;**71**:39-52. DOI: 10.1080/ 00986448808940413

[22] Hajji A, Worek WM. Simulation of a regenerative, closed-cycle adsorption cooling/heating system. Energy. 1991; **16**:643-654. DOI: 10.1016/0360-5442 (91)90035

[23] Alam KCA, Saha B, Kang YT, Akisawa A, Kashiwagi T. Heat exchanger design effect on the system performance of silica gel adsorption refrigeration systems. International Journal of Heat and Mass Transfer. 2000;**43**:4419-4431. DOI: 10.1016/ S0017-9310(00)00072-7

[24] Sun LM, Amar NB, Meunier F. Numerical study on coupled heat and mass transfer in an adsorber with external fluid heating. Heat Recovery Systems & CHP. 1995;**15**:19-29. DOI: 0890-4332(94)E0011-8

[25] Amar NB, Sun LM, Meunier F. Numerical analysis of adsorptive temperature wave regenerative heat pump. Applied Thermal Engineering. 1996;**16**:405-418. DOI: 10.1016/ 1359-4311(95)00045-3

[26] Solmuş İ, Rees DAS, Yamalı C, Baker D, Kaftanoğlu B. Numerical investigation of coupled heat and mass transfer inside the adsorbent bed of an adsorption cooling unit. International Journal of Refrigeration. 2012;**35**: 652-662. DOI: 10.1016/j.ijrefrig.2011. 12.006

[27] Solmuş İ, Yamalı C, Yıldırım C, Bilen K. Transient behavior of a cylindrical adsorbent bed during the adsorption process. Applied Energy. 2015;**142**:115-124. DOI: 10.1016/j. apenergy.2014.12.080

[28] Çağlar A, Yamalı C, Baker DK. Two dimensional transient coupled analysis of a finned tube adsorbent bed for a thermal wave cycle. International Journal of Thermal Sciences. 2013;**73**: 58-68. DOI: 10.1016/j.ijthermalsci.2013. 06.009

[29] Çağlar A. The effect of fin design parameters on the heat transfer enhancement in the adsorbent bed of a thermal wave cycle. Applied Thermal Engineering. 2016;**104**:386-393. DOI: 10.1016/j.applthermaleng.2016.05.092

[30] Li XH, Hou XH, Zhang X, Yuan ZX. A review on development of adsorption

cooling—Novel beds and advanced cycles. Energy Conversion and Management. 2015;**94**:221-232. DOI: 10.1016/j.enconman.2015.01.076

[31] COMSOL Inc. COMSOL Multiphysics Software Package Including the CFD, Heat Transfer and Chemical Reaction Engineering Modules. Version 5.2. 2017

[32] Aristov Y, Tokarev M, Freni A, Glaznev I. Kinetics of water adsorption on silica Fuji Davison RD. Microporous and Mesoporous Materials. 2006;**96**: 65-71. DOI: 10.1016/j. micromeso.2006.06.008

[33] Chihara K, Suzuki M. Air drying by pressure swing adsorption. Journal of Chemical Engineering of Japan. 1983;**16**: 293-299. DOI: 10.1252/jcej.16.293

[34] Reid RC, Prausnitz JM, Sherwood TK. Properties of Gases and Liquids. 3rd ed. New York, DC: McGraw-Hill; 1977. ISBN 978-007051790-5

[35] Solmuş İ, Yamalı C, Kaftanoğlu B, Baker D, Çağlar A. Adsorption properties of a natural zeolite–water pair for use in adsorption cooling cycles. Applied Energy. 2010;**87**:2062-2067. DOI: 10.1016/j.apenergy.2009.11.027

[36] Patankar SV. Numerical Heat Transfer and Fluid Flow. 1st ed. New York, DC: Hemisphere Publishing Corporation; 1980. 210 p. DOI: 10.1002/cite.330530323